

Holography Transformer

Chanyong Park^{a1}, Sejin Kim^{b2} and Jung Hun Lee^{b3}

^a *Department of Physics and Photon Science, Gwangju Institute of Science and Technology, Gwangju 61005, Korea*

^b *College of General Education, Kookmin University, Seoul, 02707, Korea*

ABSTRACT

We have constructed a generative artificial intelligence model to predict dual gravity solutions when provided with the input of holographic entanglement entropy. The model utilized in our study is based on the transformer algorithm, widely used for various natural language tasks including text generation, summarization, and translation. This algorithm possesses the ability to understand the meanings of input and output sequences by utilizing multi-head attention layers. In the training procedure, we generated pairs of examples consisting of holographic entanglement entropy data and their corresponding metric solutions. Once the model has completed the training process, it demonstrates the ability to generate predictions regarding a dual geometry that corresponds to the given holographic entanglement entropy. Subsequently, we proceed to validate the dual geometry to confirm its correspondence with the holographic entanglement entropy data.

¹e-mail : cyong21@gist.ac.kr

²e-mail : sejin817@kookmin.ac.kr

³e-mail : junghun.lee@kookmin.ac.kr

1 Introduction

Quantum gravity offers a unified perspective on gravity and quantum mechanics. Among various approaches, the AdS/CFT correspondence has emerged as a promising candidate for describing the interplay between these fundamental theories. This correspondence is an idea that suggests the information of quantum states can be encoded in higher-dimensional space-time [1–11], with an additional holographic coordinate that represents the energy scale in the holographic renormalization group (RG) flow [12–14].

The AdS/CFT correspondence has been extensively employed in research across various fields of physics [15–20]. Notably, Ryu and Takayanagi made a significant achievement by introducing a method to calculate entanglement entropy in holography [9], overcoming the complexity associated with theoretical approaches. Their work opened new avenues for exploration in quantum field theory [19–24].

Artificial intelligence (AI) has recently played a crucial role in enhancing our understanding of holography theory. Deep learning techniques, especially when applied to the analysis of strongly-coupled systems, have proven invaluable [25–33]. Deep neural networks have demonstrated their prowess in predicting and understanding condensed matter systems [26].

This paper introduces AI methods for reconstructing dual geometries by analyzing holographic entanglement entropies. Our method aims to reconstruct theories or equations of motion from experimental or observational data, which is a formidable challenge due to the nonlinear nature of the equations that govern quantum theory and gravity.

To reconstruct holography theories from experimental results, it is necessary to accurately analyze and understand the correlations between the data. One has reconstruct dual geometries from entanglement entropy by developing lattice method in [34, 35]. We will utilize the transformer algorithm, a powerful artificial intelligence tool that can comprehend important information from data and generate new insights.

In this paper, we present a novel approach where we employ the transformer algorithm to predict gravity solutions that satisfy asymptotic AdS boundary conditions and have holographic entanglement data within the framework of holography theory in both three and four dimensions. The transformer model we constructed establishes connections between sequences of holographic entanglement entropies and their dual geometries, predicting gravity solutions that satisfy our metric ansatz.

The paper is organized as follows. In section 2, we introduce the basic concept of the transformer AI and explain how the model works in detail. We provide an overview of holography theory for calculating entanglement entropy. In section 3, we verify our transformer model using the three- and four-dimensional charged p-brane black hole geometries. In section 4, we feed the transformer model with the holographic entanglement entropy data of unknown dual geometries in three and four dimensions. We compute holographic entanglement entropy using the prediction to verify the performance of the transformer model. Finally, we conclude this work with some final remarks in section 5.

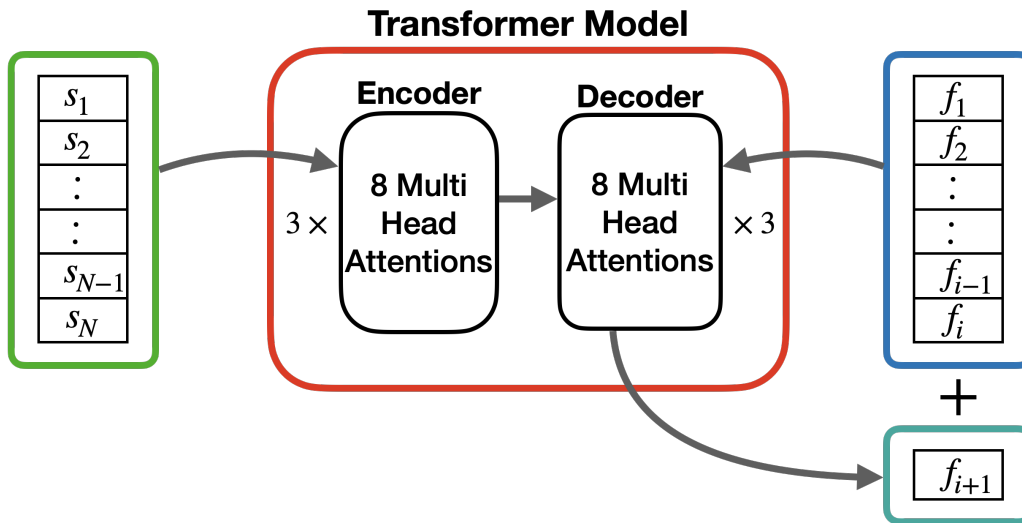


Figure 1: This figure illustrates the structure of the transformer model used to extract information about holographic dual geometry from entanglement entropy data.

2 Transformer AI

The generative transformer model is a neural network architecture commonly used in natural language processing tasks, such as language translation and text summarization. The generative transformer model was first introduced by [36] and has since become widely utilized in various natural language applications [37–40]. They are not limited to natural language processing alone but have also found applications in computer vision and scientific research [41–43].

The transformer model consists of two main components which are the encoder and the decoder block. The primary role of the encoder block is to comprehend information from the input sequence, while the decoder block generates the next output sequence based on the encoded information and the output sequence in Fig.(1). Since the input shape and output shape of the encoder and decoder are the same, we can stack encoder and decoder to improve the performance of the transformer model.

Both the encoder and decoder blocks in the transformer model include a multi-head self-attention layer. This layer takes three inputs, query, key, and value. The attention layer utilizes dot product and softmax function to calculate the similarities between the query and key, enabling it to comprehend language and generate coherent output.

$$\text{Attention} = V \text{ Softmax} \left(\frac{Q \cdot K}{\sqrt{d_k}} \right), \quad (1)$$

where Q , K and V represent the query, key and value, and d_k is the dimension of the transformer model.

In this paper, we have constructed a generative transformer model as shown in Fig.(1), designed to predict the dual geometry from holographic entanglement entropy data. Our transformer model consists of three decoders and three encoders. Here, we use 8 attention heads for

both the encoder and decoder layers. In Fig.(1), the input data in the green box is a sequence of derivatives of holographic entanglement entropy with respect to the boundary size l , and the output in the blue box is a sequence corresponding to the dual geometry of the input data.

$$s_i = \partial_l S|_{l=l_i}, \quad f_i = f(z_i). \quad (2)$$

The derivative of entanglement entropy is considered as the Hamiltonian of the minimal surface action. The Hamiltonian contains sufficient geometric information for reconstruction and can avoid dependence on the UV cutoff. It is considered as part of managing the input dataset.

In Fig.(1), generative transformers typically operate with an encoder that analyzes the input sequence and a decoder that analyzes the information received from the encoder, along with the output data, to make predictions for the next output value. Similar to model like chat GPT, in natural language tasks, we utilize tokens such as $\langle sos \rangle$ (start of sequence) to initiate the process and continue until we reach the $\langle eos \rangle$ (end of sequence) token. This allows us to generate predictions for the dual geometry.

The transformer model is a generative artificial intelligence model designed to generate new data that is similar to a given dataset. These models learn the underlying patterns and structures within a dataset and can produce new, original data samples that share characteristics with the training data. Our model takes an input and output sequence and generates the next output sequence, denoted as f_{n+1} , until it reaches the end of sequence token $\langle eos \rangle$ such as

$$\text{Transformer}(|sos, s_1, \dots, s_n, \dots, s_N, eos\rangle, |sos, f_1, \dots, f_n\rangle) = |f_{n+1}\rangle. \quad (3)$$

In this paper, we used cross entropy loss as the criterion and the Adam method as the optimizer to train the generative model.

Once the transformer model is trained, we utilize it to predict the dual geometry from holographic entanglement entropy data and experimental results. The trained model should provide results that align with the metric ansatz we have considered, given that the transformer model has been trained using data within this ansatz. Since holographic entanglement entropy is defined as the area of the minimal surface [9], we can verify whether the predictions of the transformer model accurately represent the dual geometry.

In [31], holographic entanglement entropy of black holes was investigated using a deep learning approach. Transformer models typically require a large amount of data to optimize themselves. However the time spent on data generation and training is significantly less than that required for the deep learning method. This is primarily because deep learning models, especially those with a large number of layers, demand extensive computational resources to improve their accuracy.

Let us enumerate several advantages of the transformer model over traditional deep learning models in the context of evaluating holographic entanglement entropy

1. Unlike deep learning models, which rely on implicitly incorporating holography formulas, transformer models do not require prior knowledge of how to evaluate holographic entanglement entropy. They learn to extract relevant information directly from the data.
2. Deep learning requires iterative repeated optimization to obtain dual geometry, whereas transformer models simply learn from training data that includes both holography data

and dual geometries. The transformer model immediately provides a dual geometry from holographic entanglement entropy data.

3. Deep learning methods often struggle with the singularity present in the integrand of the holographic entanglement entropy formula, making it challenging to accurately capture the size of the black hole horizon. In contrast, transformer models are not encumbered by singularities and can provide an accurate determination of the black hole horizon size.
4. In deep learning methods, the loss function includes an L1 norm to impose smoothness in the blackening factor, which can inevitably occur numerical errors. Transformer models do not depend on this norm and can avoid such issues, leading to more precise results.

In [26, 31], deep learning consists of specific neural layers, allowing one to understand the mechanism of how the model learns and works. The transformer model, however, is an ordinary artificial neural network model and its internal structure is often considered a black box. We followed the guideline of [44] to train our transformer model.

2.1 Data Generate

We will generate data to train a generative transformer model to predict dual geometries from holographic entanglement entropy data. Unlike deep learning methods [31], we will not provide any theoretical or physical information to the transformer model, but instead, we will only supply answers corresponding to the holographic entanglement data's dual geometry. The data generation process is based on the principles of holography theory.

We are considering a holographic dual of d -dimensions quantum field theory. And we will reconstruct the geometry solution of holographic dual which having the holographic entanglement entropy what we are interested in. Let's assume that the simple metric ansatz is given by

$$ds^2 = \frac{R^2}{z^2} \left(-g(z)dt^2 + \frac{dz^2}{f(z)} + \sum_{i=1}^{d-1} dx_i^2 \right), \quad (4)$$

here, the constant R is a radius of AdS space. The function g and f should approach 1 as $z \rightarrow 0$ since we are considering asymptotic AdS space. In general, there is no reason for the functions g and f to be the same. In this paper, we use a time-independent entanglement entropy formula, therefore it's impossible to determine g . To determine g , one would need either time-dependent entanglement entropy data or information about the matter field.

For strip-shaped subregion A , the entanglement entropy is given by the area of the minimal surface which is homologous to the subregion A ,

$$S = \frac{R^{d-1} \text{Vol}(\mathbb{R}^{d-2})}{4G_{d+1}} \int_{-l/2}^{l/2} dx_1 \frac{1}{z^{d-1}} \sqrt{1 + \frac{(z')^2}{f}}, \quad (5)$$

where $\text{Vol}(\mathbb{R}^{d-2})$ is the renormalized volume of the spatial directions orthogonal to x_1 on the d -dimensional AdS boundary. Since the translational symmetry along the coordinate x_1 , the following Hamiltonian constraint simplifies the integrand of the area functional (5),

$$H = -\frac{R^{d-1}\text{Vol}(\mathbb{R}^{d-2})}{4G_{d+1}} \frac{1}{z^{d-1}} \left(1 + \frac{(z')^2}{f}\right)^{-1/2} = -\frac{R^{d-1}\text{Vol}(\mathbb{R}^{d-2})}{4G_{d+1}} \frac{1}{z_t^{d-1}}, \quad (6)$$

where z_t is a turning point when $dz/dx = 0$ and a function of l . Using Hamiltonian constraint, boundary size l and holographic entanglement entropy can be defined by integrate under z ,

$$l = \int_0^{z_t} dz \frac{2z^{(d-1)}}{\sqrt{f}\sqrt{z_t^{2(d-1)} - z^{2(d-1)}}},$$

$$S = \frac{R^{d-1}\text{Vol}(\mathbb{R}^{d-2})}{2G_{d+1}} \left(\frac{l}{2z_t^{d-1}} + \frac{1}{z_t^{d-1}} \int_0^{z_t} dz \frac{\sqrt{z_t^{2(d-1)} - z^{2(d-1)}}}{z^{(d-1)}\sqrt{f}} \right). \quad (7)$$

By using Leibniz integral rule, one can easily evaluate the derivative of holographic entanglement entropy with respect the boundary size l is obtained by

$$\frac{dS}{dl} = \frac{R^{d-1}\text{Vol}(\mathbb{R}^{d-2})}{4G_{d+1}z_t^{d-1}}. \quad (8)$$

Here using chain rule, the derivative of S_{EE} with respect z_t becomes to zero by the definition of boundary size l . In classical mechanics, the result is obvious because it is nothing more Hamilton-Jacobi equation and the time derivative of onshell action gives the Hamiltonian. In this paper, we use a value of 1 for a constant known as $R^{d-1}/2G_{d+1}$ to simplify the calculations.

Unlike a disk shape, the holographic entanglement entropy of the strip subregion has translation symmetry under x_1 and the Hamiltonian. We can evaluate the relation between the Hamiltonian, rewritten in terms of the turning point, and the boundary size l when the derivative of entropy is given. This task reduces to figuring out the function f from the integration with a weight function,

$$l = \int_0^{z_t} dz \frac{2z^{(d-1)}}{\sqrt{f}\sqrt{z_t^{2(d-1)} - z^{2(d-1)}}} \equiv \left\langle \frac{1}{\sqrt{f}} \right\rangle_d. \quad (9)$$

To train the transformer model, we utilize a data generator to create holographic examples using holography theory. The data generator takes a metric solution's blackening factor $f(z)$ as input and provides the sequence of the derivative of holographic entanglement entropy as output,

$$\text{Generator}(f(z)) = \{\text{input} : |sos, s_1, \dots, s_N, eos\rangle, \text{output} : |sos, f_1, \dots, f_N, eos\rangle\}. \quad (10)$$

Here, s_i and f_i represent $dS/dl|_{l=\Delta i+\epsilon}$ and $f(\Delta i)$ where ϵ is a cutoff to avoid diverge of data and Δ the size of the interval to determine maximum sentence length. We randomly generated arbitrary metric solutions and evaluated example pairs using the data generator.

3 Black hole Geometries

As a simple model, we first consider the BTZ black hole without charge. For this case, it is well known that the entanglement entropy has the analytic form

$$S = \frac{R}{2G_3} \log \left(\frac{2z_h}{\epsilon} \sinh \left(\frac{l}{2z_h} \right) \right), \quad (11)$$

where z_h denotes the black hole horizon, and ϵ is a UV cutoff which introduced to regulate the divergence arising at the boundary. Conversely, in the case of the charged BTZ black hole, the entanglement entropy does not have an analytic expression.

Our transformer model comprises three encoders and three decoders. To train our model, we utilize entanglement entropy data from a three-dimensional p-brane black hole with a charge [45, 46] as input and generate a dataset using a random metric solution, resulting in a total of 135,232 example pairs. The data generator for our 3D black hole transformer model takes the blackening factor, denoted as $f(z)$, and produces corresponding input and output sequences defined as follows,

$$\text{Generator}(f(z)) = \{\text{input} : |sos, s_1, \dots, s_N, eos\rangle, \text{output} : |sos, f_1, \dots, f_N, eos\rangle\}, \quad (12)$$

where

$$\begin{aligned} |sos, s_1, \dots, s_N, eos\rangle &= \left\{ s_i = l(z_t = \Delta i + \epsilon) \left| \frac{R}{4G_3 z_t} = \frac{dS(l; f)}{dl} \right. \right\}, \\ |sos, f_1, \dots, f_N, eos\rangle &= \left\{ f_i = f(z = \Delta i) \left| f(z) = 1 - \rho z - M z^2 + \frac{Q^2}{2} z^2 \log(z) \right. \right\}. \end{aligned} \quad (13)$$

Here, we set the coefficients ρ , M , and Q to follow a normal distribution with a mean value of $m = 0$ and a variance of $\sigma = 1$, while gathering examples where $z_h < 3$.

The length of both input and output sequences is determined by the values of Δ and ϵ , which are set to $\Delta = 0.01$ and $\epsilon = 0.1$. The value of N depends on the black hole horizon z_h and the blackening factor f , resulting in varying sequence lengths for each example. Since we impose the condition $z_h < 3$, the maximum sequence length is less than 300.

It's important to note that our transformer model only accepts integer values for input and output data. To achieve this, we round the s_i and f_i values to four effective numbers. If one desires higher accuracy in the transformer model, it's necessary to increase the tokenizer size and, consequently, the overall model size.

To prevent the possibility of a transformer model manipulating future text, we apply a padding mask. This mask assigns a value to specific positions within the output sequence, as given by

$$|sos, f_1, \dots, f_N, eos\rangle \rightarrow |sos, f_1, \dots, f_i, mask, \dots, mask, eos\rangle. \quad (14)$$

This technique is widely employed in natural language tasks and serves to guide the transformer model in generating new sequences.

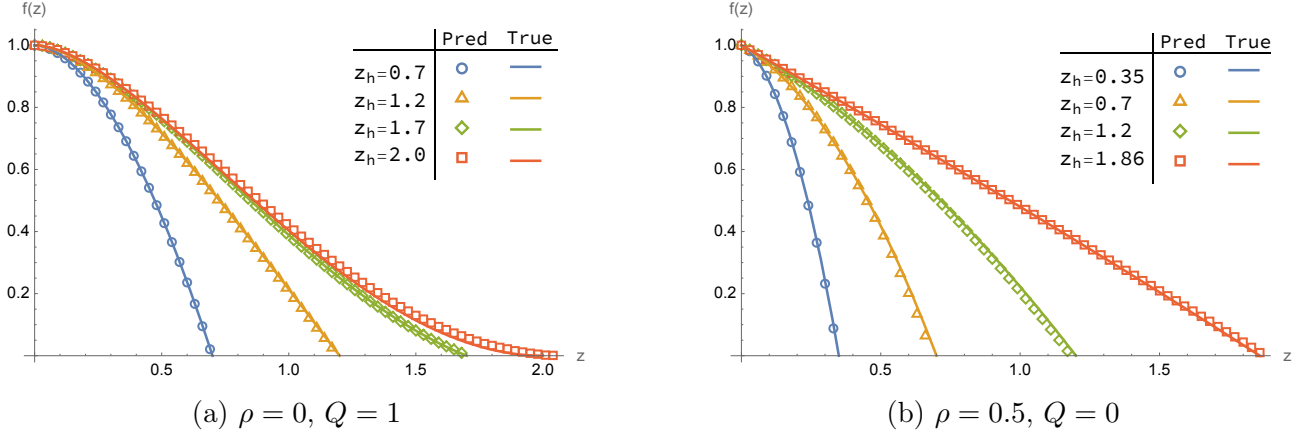


Figure 2: In these figures, lines and shapes represent the true values and model prediction results, respectively.

3.1 3 Dimensional Black Hole

The trained model demonstrates a remarkable ability to predict the geometries of charged black holes from holographic entanglement entropy. In Fig.(2a), we can observe the surface representing the predictive metric of holographic entanglement entropy as the parameter changes. The Fig.(2a) illustrates the variation of the blackening factor $f(z)$ while keeping the charge fixed at $Q = 1$, as the black hole horizon z_h changes.

An interesting example worth mentioning is the use of p-brane gas geometry to evaluate the performance of the transformer model. In a recent study by [12], they investigated p-brane gas geometry and its associated thermodynamics. The p-brane gas geometry is characterized by an exact form, and its blackening factor can be expressed as

$$f = 1 - \rho z - Mz^2, \quad (15)$$

where M and ρ represent the black hole mass and the density of the brane, respectively.

The holographic entanglement entropy S of the p-brane gas geometry does not have an exact result, but it can be evaluated using (7). The resulting entanglement entropy should be a function of z_h and ρ . To test the trained model, the cases of p-brane gas geometry are considered in Fig.(2b), where ρ is fixed while the black hole horizon changes.

3.2 Four dimensions black hole Geometries

We attempted to predict a dual geometry in 4D using a transformer model with the same structure as the one designed for 3D. During training, the model was trained on a dataset consisting of 152,740 samples, with a specific focus on the holographic entanglement entropy of charged p-brane Reissner–Nordström (RN) black holes. The training data generator for our 4D black hole transformer model is defined as follows,

$$\text{Generator}(f(z)) = \{\text{input} : |sos, s_1, \dots, s_N, eos\rangle, \text{output} : |sos, f_1, \dots, f_N, eos\rangle\}, \quad (16)$$

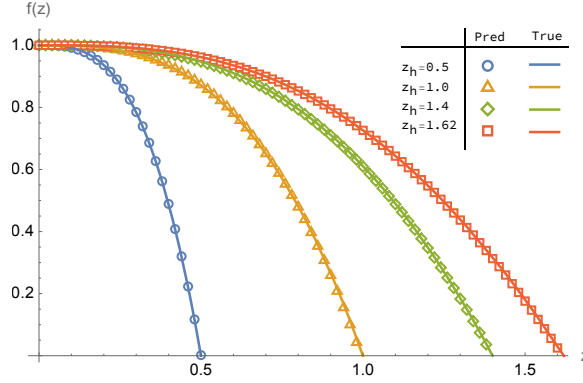


Figure 3: The figure corresponds to the case where $\rho = 0$, $Q = 0.5$, and z_h is varied within the range 0.5, 1, 1.4, 1.62. The lines and shapes in these figures represent the true dual geometries and predictions of the transformer model.

where

$$\begin{aligned}
 |sos, s_1, \dots, s_N, eos\rangle &= \left\{ s_i = l(z_t = \Delta i + \epsilon) \left| \frac{R}{4G_3 z_t} = \frac{dS(l; f)}{dl} \right. \right\}, \\
 |sos, f_1, \dots, f_N, eos\rangle &= \left\{ f_i = f(z = \Delta i) \left| f(z) = 1 - \rho z^2 - M z^3 + \frac{Q^2}{4} z^4 \log(z) \right. \right\}. \quad (17)
 \end{aligned}$$

Here, the constants ρ , M , and Q are determined in the same way as in the 3D case.

The RN black hole geometry is a well-known charged black hole in four dimensions. This specific charged black hole in four dimensions is described by the equation,

$$f(z) = 1 - M z^3 + \frac{Q^2 z^4}{4R^2}. \quad (18)$$

However, there is currently no exact solution available for the holographic entanglement entropy of the RN black hole. To evaluate the performance of our four-dimensional transformer model, we conducted experiments, the results of which are presented in Fig.(3).

4 Unknown Dual Geometry

In this section, we assess the performance of our transformer model in predicting outcomes for both 3D and 4D cases, specifically regarding holographic entanglement entropy data associated with unknown dual geometries. We validate the transformer model by comparing the input data with the evaluated holographic entanglement entropy, which can be predicted using the model.

In [31], a dual geometry was reconstructed using a deep learning method to calculate holographic entanglement entropy. One of the analyzed forms is given as follows,

$$S(l) = \frac{R}{2G_3} \log \left(\frac{2a}{\epsilon} \left(\exp \left(\frac{l}{2a} \right) - 1 \right) \right), \quad (19)$$

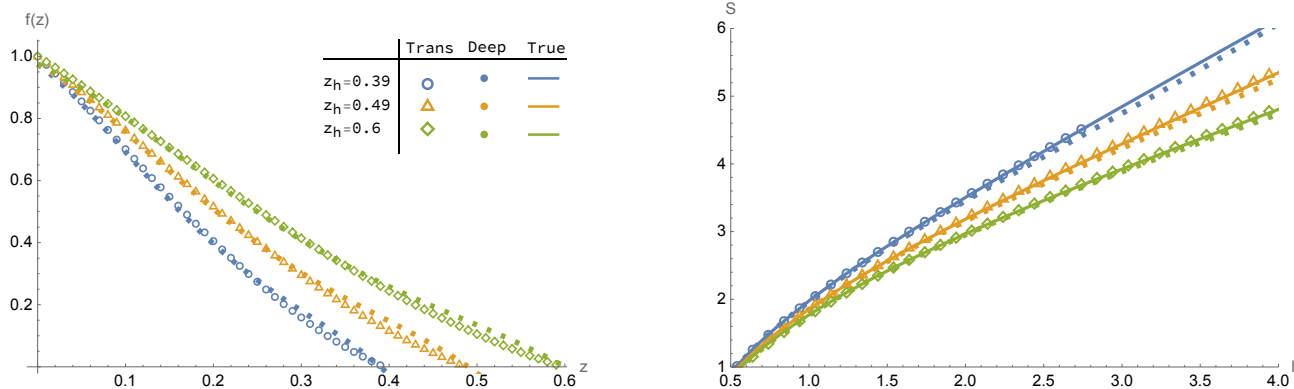


Figure 4: These figures present dual geometry predictions of transformer and deep learning models in [31] for holographic entanglement entropy data in (19) at different values of $z_h = 0.39, 0.49, 0.6$. The left figure shows results obtained using the transformer and deep learning methods, while the right figure provides a comparison between the holographic entanglement entropy evaluated by the transformer, deep learning, and the input data.

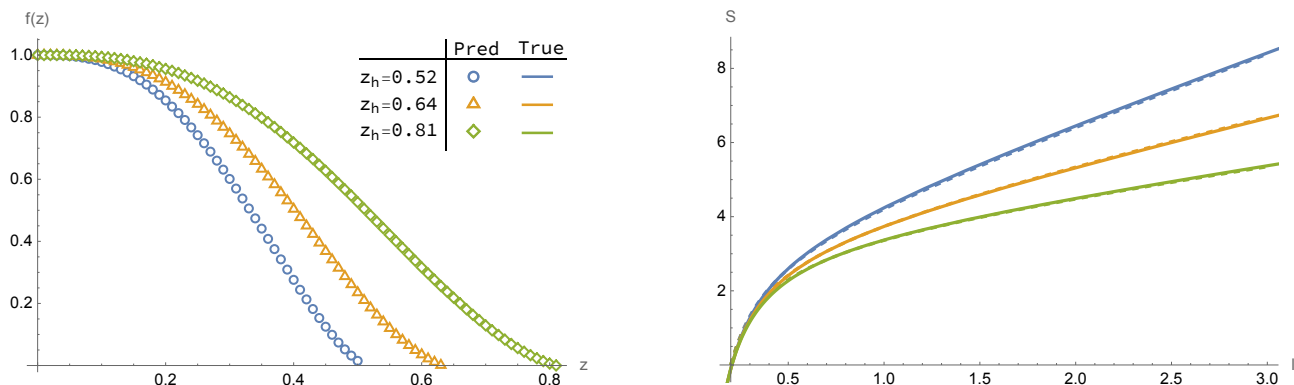


Figure 5: Dual geometries and holographic entanglement entropy for (21). The left figure represents predictions generated by the transformer model for different values of $z_h = 0.52, 0.64, 0.81$, while the right figure provides a comparison between the holographic entanglement entropy evaluated by the model prediction and the input data.

Here, the parameter a plays the role of the black hole horizon. In the IR limit, as $l \rightarrow \infty$, expression (19) yields the thermal entropy,

$$S_{TH} = \frac{R}{4G_3} \frac{l}{a}, \quad a = z_h. \quad (20)$$

And it also recovers the entanglement entropy of pure AdS geometry in the UV limit.

Our trained transformer model can predict a dual geometry based on provided holographic entanglement entropy data. The right side in Fig.(4) displays the holographic entanglement entropy obtained using the predicted blackening factor generated by the transformer model. This transformer model can accurately predict the holographic entanglement entropy based on the provided data, enabling continuous predictions that are not achievable with deep learning methods.

We have developed a transformer model designed to predict dual geometries. Furthermore, our research objective involves determining the dual geometry associated with holographic entanglement entropy. We consider a specific entropy described by the following expression,

$$S = \frac{R^2}{2G_4} \left(-\frac{AGM(\sqrt{2}, 1)^2}{2} \frac{1}{l} + \frac{l}{2z_h^2} \right). \quad (21)$$

Here, the function $AGM(\sqrt{2}, 1)$ represents the Arithmetic-Geometric Mean function and can be expressed as $(2\pi)^{3/2} / \Gamma(\frac{1}{4})^2$. This function is derived from the pure AdS case.

In Fig.(5), we present the results obtained using our trained transformer model for 4D, predicting the dual geometry for the holographic entanglement entropy described in (21). Since the dual geometry is currently unknown, we have reevaluated the holographic entanglement entropy and compared the resulting values with our input data.

The transformer model can immediately predict the dual geometry from holographic entanglement entropy data. This allows us to understand the behavior of the blackening factor f for verifying parameters like z_h . The thermal temperature is one of the most interesting physical quantities for understanding black holes and holographic thermal systems. It is evaluated from the derivative of f as given by,

$$T_H = -\frac{f'(z_h)}{4\pi}. \quad (22)$$

Using the trained transformer model, we determine the temperature of the dual geometry for the unknown case in Fig.(6). The gray dashed lines represent fitting functions, and we have identified the following expressions,

$$\begin{aligned} T_H^{3D} &= \frac{1}{2\pi z_h} - \frac{0.237262}{z_h^2} + \frac{0.175508}{z_h^3} - \frac{0.0577989}{z_h^4} + \frac{0.00708551}{z_h^5}, \\ T_H^{4D} &= \frac{3}{4\pi z_h} - \frac{0.276375}{z_h^2} + \frac{0.0957488}{z_h^3}. \end{aligned} \quad (23)$$

These fitting functions are based on the inverse Gaussian function to accurately fit the data. These expressions are obtained using GeneralizedLinearModelFit in Mathematica. The first term is fixed and depends on the dimension when we consider the low-temperature limit, which means that the size of the black hole horizon approaches zero.

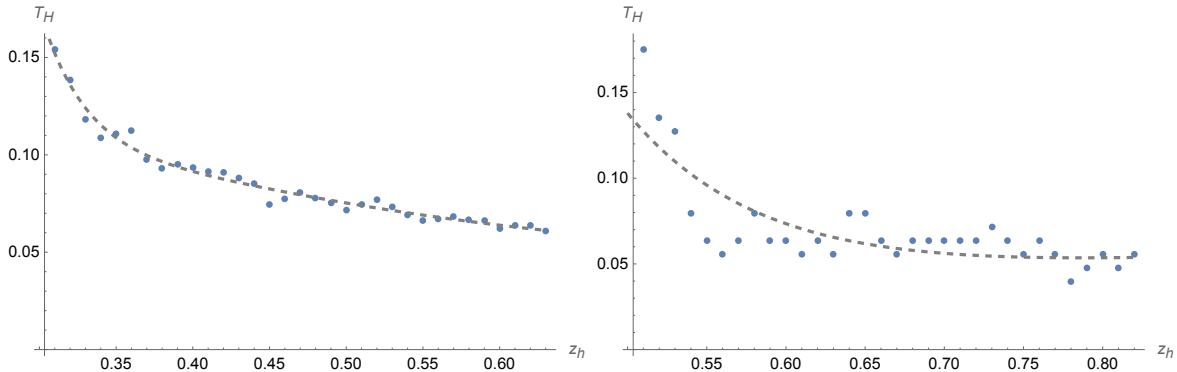


Figure 6: These figures present the thermal temperature of unknown 3D and 4D black holes. The left figure is for the 3D case, and the right figure is for the 4D case. The gray dashed lines represent fitting functions in (23).

5 Discussion

In this study, we have developed a transformer model to reconstruct dual geometries by analyzing holographic entanglement entropies. Originally designed for natural language tasks such as translation, summarization, sentence completion, and more, the transformer model has demonstrated its ability to understand sentence meaning and generate new words using a large language model. Furthermore, it is now being applied to tasks such as vision recognition and numerical simulations due to its performance. The model can even tackle tasks that lack a mathematical relationship between input and output sequences.

We presented an application of a transformer model in deriving gravitational solutions from input data of non-local physical quantities. To model it, we considered the input data of two- and three-dimensional entanglement entropy. The dataset generator, which follows the principles of holography theory, takes a randomly generated metric solution $f(z)$ and provides sequences of the derivative of entropy as input and values of f as output. Using this approach, we generate over 100,000 pairs of examples for three- and four-dimensional charged p-brane black holes.

In this paper, our transformer model was not provided with any information regarding holography theory, smoothness, or asymptotic AdS boundary conditions. Nevertheless, the trained transformer produces a smooth dual geometric solution that satisfies asymptotic AdS boundary conditions and generates input data for holographic entanglement entropy. We also observed that our model has the capability to generate new holographic geometries from previously unknown input data.

We noticed that the performance of the transformer model improves with larger example sizes. It is well-known that the transformer model's performance depends on both model size and example size. A small number of examples is insufficient for training a large model, and using a large model can easily lead to overfitting during the learning process.

This method can be applied to construct complex holography and quantum theory from physical observations and phenomena. Reconstructing dual geometry is the inverse process of a

non-invertible calculation. Holographic entanglement entropy is evaluated using an integration formula with varying initial values. This process is analogous to determining the potential and external forces acting on a moving particle. If the transformer model studies the interaction patterns between particles and fields, it can provide explanations for physical phenomena by modeling their interactions.

We will develop a transformer model that predicts holographic entanglement entropy with a disk boundary. Entanglement entropy within a disk is more closely related to real-world phenomena and experimental systems. However, the disk case breaks translation symmetry, and the derivative of entropy alone is insufficient to capture all the information about dual geometry.

Acknowledgement

Sejin Kim thanks to Yunseok Seo for supporting research. C. Park was supported by the National Research Foundation of Korea(NRF) grant funded by the Korea government(MSIT) (No. NRF-2019R1A2C1006639). J. H. Lee was supported by the National Research Foundation of Korea(NRF) grant funded by the Korea government(MSIT) (No. NRF-2021R1C1C2008737).

References

- [1] J. M. Maldacena, *Int. J. Theor. Phys.* **38**, 1113 (1999), [Adv. Theor. Math. Phys.2,231(1998)], [arXiv:hep-th/9711200 \[hep-th\]](#) .
- [2] S. S. Gubser, I. R. Klebanov, and A. M. Polyakov, *Phys. Lett. B* **428**, 105 (1998), [arXiv:hep-th/9802109](#) .
- [3] E. Witten, *Adv.Theor.Math.Phys.* **2**, 253 (1998), [hep-th/9802150](#) .
- [4] E. Witten, *Adv.Theor.Math.Phys.* **2**, 505 (1998), [hep-th/9803131](#) .
- [5] O. Aharony, S. S. Gubser, J. M. Maldacena, H. Ooguri, and Y. Oz, *Phys. Rept.* **323**, 183 (2000), [arXiv:hep-th/9905111 \[hep-th\]](#) .
- [6] S. de Haro, S. N. Solodukhin, and K. Skenderis, *Commun. Math. Phys.* **217**, 595 (2001), [arXiv:hep-th/0002230](#) .
- [7] M. Benna, I. Klebanov, T. Klose, and M. Smedback, *JHEP* **09**, 072 (2008), [arXiv:0806.1519 \[hep-th\]](#) .
- [8] O. Bergman, D. Rodríguez-Gómez, and C. F. Uhlemann, *JHEP* **08**, 127 (2018), [arXiv:1806.07898 \[hep-th\]](#) .
- [9] S. Ryu and T. Takayanagi, *JHEP* **08**, 045 (2006), [arXiv:hep-th/0605073 \[hep-th\]](#) .
- [10] B. Swingle, *Phys. Rev. D* **86**, 065007 (2012), [arXiv:0905.1317 \[cond-mat.str-el\]](#) .

- [11] R. Mojtahedi, M. Hamghalam, R. K. G. Do, and A. L. Simpson, in *Multiscale Multimodal Medical Imaging* (Springer Nature Switzerland, 2022) pp. 110–120.
- [12] C. Park, S.-J. Kim, and J. H. Lee, (2022), [2212.01214](#) .
- [13] C. Park and J. H. Lee, *Phys. Rev. D* **101**, 086008 (2020), [1910.05741](#) .
- [14] C. Park, D. Ro, and J. H. Lee, (2018), [10.1007/JHEP11\(2018\)165](#), [1806.09072](#) .
- [15] J. Erlich, E. Katz, D. T. Son, and M. A. Stephanov, *Phys. Rev. Lett.* **95**, 261602 (2005), [arXiv:hep-ph/0501128](#) .
- [16] A. Karch, E. Katz, D. T. Son, and M. A. Stephanov, *Phys. Rev. D* **74**, 015005 (2006), [arXiv:hep-ph/0602229](#) .
- [17] A. Karch and E. Katz, *JHEP* **06**, 043 (2002), [arXiv:hep-th/0205236](#) .
- [18] H. Casini, M. Huerta, and R. C. Myers, *JHEP* **05**, 036 (2011), [arXiv:1102.0440 \[hep-th\]](#) .
- [19] T. Faulkner, A. Lewkowycz, and J. Maldacena, *JHEP* **11**, 074 (2013), [arXiv:1307.2892 \[hep-th\]](#) .
- [20] R. C. Myers and A. Sinha, *JHEP* **01**, 125 (2011), [arXiv:1011.5819 \[hep-th\]](#) .
- [21] J. Maldacena and L. Susskind, *Fortsch. Phys.* **61**, 781 (2013), [arXiv:1306.0533 \[hep-th\]](#) .
- [22] A. Lewkowycz and J. Maldacena, *JHEP* **08**, 090 (2013), [arXiv:1304.4926 \[hep-th\]](#) .
- [23] T. Nishioka, S. Ryu, and T. Takayanagi, *J. Phys. A* **42**, 504008 (2009), [arXiv:0905.0932 \[hep-th\]](#) .
- [24] G. Penington, *JHEP* **09**, 002 (2020), [arXiv:1905.08255 \[hep-th\]](#) .
- [25] Y.-Z. You, Z. Yang, and X.-L. Qi, *Physical Review B* **97** (2018), [10.1103/physrevb.97.045153](#).
- [26] K. Hashimoto, S. Sugishita, A. Tanaka, and A. Tomiya, *Phys. Rev. D* **98**, 046019 (2018), [1802.08313](#) .
- [27] S. Shiba Funai and D. Giataganas, *Phys. Rev. Res.* **2**, 033415 (2020), [arXiv:1810.08179 \[cond-mat.stat-mech\]](#) .
- [28] T. Akutagawa, K. Hashimoto, and T. Sumimoto, *Phys. Rev. D* **102**, 026020 (2020), [2005.02636](#) .
- [29] S. Y. Chen, H. T. Ding, F. Y. Liu, G. Papp, and C. B. Yang, (2021), [arXiv:2110.13521 \[hep-lat\]](#) .
- [30] J. Lam and Y.-Z. You, *Phys. Rev. Res.* **3**, 043199 (2021), [arXiv:2110.01115 \[hep-th\]](#) .

- [31] C. Park, C.-O. Hwang, K. Cho, and S.-J. Kim, *Phys. Rev. D* **106**, 106017 (2022), [arXiv:2205.04445 \[hep-th\]](#) .
- [32] K. Li, Y. Ling, P. Liu, and M.-H. Wu, *Phys. Rev. D* **107**, no.6, 066021 (2023), [2209.05203](#) .
- [33] Y.-Z. You, Z. Yang, and X.-L. Qi, *Phys. Rev. B* **97**, 045153 (2018), [arXiv:1709.01223 \[cond-mat.dis-nn\]](#) .
- [34] N. Jokela and A. Pönni, *Phys. Rev. D* **103**, 026010 (2021), [2007.00010](#) .
- [35] N. Jokela, A. Pönni, T. Rindlisbacher, K. Rummukainen, and A. Salami, (2023), [2304.08949](#) .
- [36] A. Vaswani, N. Shazeer, N. Parmar, J. Uszkoreit, L. Jones, A. N. Gomez, L. Kaiser, and I. Polosukhin, (2017), [1706.03762](#) .
- [37] T. B. Brown, B. Mann, N. Ryder, M. Subbiah, J. Kaplan, P. Dhariwal, A. Neelakantan, P. Shyam, G. Sastry, A. Askell, S. Agarwal, A. Herbert-Voss, G. Krueger, T. Henighan, R. Child, A. Ramesh, D. M. Ziegler, J. Wu, C. Winter, C. Hesse, M. Chen, E. Sigler, M. Litwin, S. Gray, B. Chess, J. Clark, C. Berner, S. McCandlish, A. Radford, I. Sutskever, and D. Amodei, (2020), [2005.14165](#) .
- [38] J. Devlin, M.-W. Chang, K. Lee, and K. Toutanova, (2018), [1810.04805](#) .
- [39] H. Touvron, T. Lavril, G. Izacard, X. Martinet, M.-A. Lachaux, T. Lacroix, B. Rozière, N. Goyal, E. Hambro, F. Azhar, A. Rodriguez, A. Joulin, E. Grave, and G. Lample, (2023), [2302.13971](#) .
- [40] OpenAI, “Gpt-4 technical report,” (2023), [arXiv:2303.08774 \[cs.CL\]](#) .
- [41] A. Dosovitskiy, L. Beyer, A. Kolesnikov, D. Weissenborn, X. Zhai, T. Unterthiner, M. Dehghani, M. Minderer, G. Heigold, S. Gelly, J. Uszkoreit, and N. Houlsby, (2020), [2010.11929](#) .
- [42] L. Qin, M. Wang, C. Deng, K. Wang, X. Chen, J. Hu, and W. Deng, (2023), <https://doi.org/10.1109/TCSVT.2023.3304724>, [2308.11509](#) .
- [43] K. Bi, L. Xie, H. Zhang, X. Chen, X. Gu, and Q. Tian, *Nature* **619**, 533 (2023).
- [44] M. Popel and O. Bojar, *The Prague Bulletin of Mathematical Linguistics* **110**, 43 (2018).
- [45] A. Chamblin, H. S. Reall, H. aki Shinkai, and T. Shiromizu, *Phys.Rev.* **D63**, 064015 (2001), [hep-th/0008177](#) .
- [46] C. Park and S.-J. Sin, *Phys.Rev.* **D57**, 4620 (1998), [hep-th/9707003](#) .